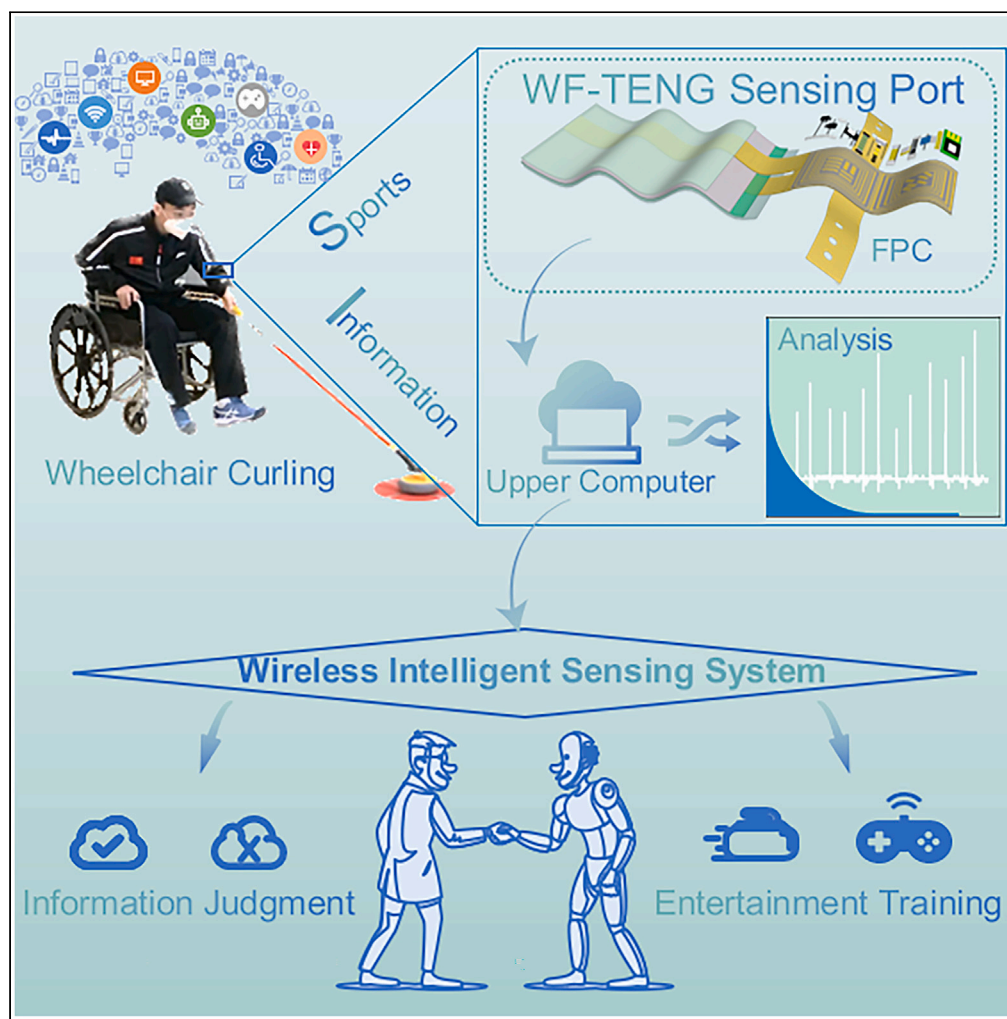


Article

Flexible wearable intelligent sensing system for wheelchair sports monitoring



Yupeng Mao,
Yuzhang Wen,
Bing Liu, ..., Zuojun
Yu, Liang Chu,
Aiguo Zhou

maoyupeng@pe.neu.edu.cn

Highlights

The fully encapsulated sensor structure ensures its stability

The wireless intelligent sensing system has excellent self-powered capability

Remote transmission of sensors provides more possibilities for monitoring

Promote the development of wearable devices in the field of sports for the disabled

Mao et al., iScience 26, 108126
November 17, 2023 © 2023 The
Author(s).
[https://doi.org/10.1016/
j.isci.2023.108126](https://doi.org/10.1016/j.isci.2023.108126)



Article

Flexible wearable intelligent sensing system for wheelchair sports monitoring

Yupeng Mao,^{1,5,6,*} Yuzhang Wen,⁵ Bing Liu,⁴ Fengxin Sun,⁵ Yongsheng Zhu,⁵ Junxiao Wang,¹ Rui Zhang,¹ Zuojun Yu,³ Liang Chu,² and Aiguo Zhou¹

SUMMARY

The application of wearable intelligent systems toward human-computer interaction has received widespread attention. It is still desirable to conveniently promote health and monitor sports skills for disabled people. Here, a wireless intelligent sensing system (WISS) has been developed, which includes two ports of wearable flexible triboelectric nanogenerator (WF-TENG) sensing and an upper computer digital signal receiving intelligent processing. The WF-TENG sensing port is connected by the WF-TENG sensor and flexible printed circuit (FPC). Due to its flexibility, the WF-TENG sensing port can be freely adhered on the surface of human skin. The WISS can be applied to entertainment reaction training based on human-computer interaction, and to the technical judgment and analysis on wheelchair curling sport. This work provides new application opportunities for wearable devices in the fields of sports skills monitoring, sports assistive devices and health promotion for disabled people.

INTRODUCTION

The World Health Organization (WHO) reminds that there are more than 65 million disabled people who use wheelchairs in the world. The number is continuously increasing due to unfortunate accidents.¹ However, wheelchair users face multiple psychological and physical disadvantages as a result of their physical disability, leading to a higher risk of obesity and cardiovascular disease.^{2–8} This group deserves more attention than a normal group in terms of emotional, physiology, social identity, and physical health.^{9–11} Taking part in physical exercise is an effective way to reduce the incidence of obesity to prevent cardiovascular and other diseases.^{12–15} Wheelchair curling sport is really interesting to wheelchair users, with the characteristics of “easy entry” and “difficult elite”. Importantly, wheelchair curling sport can be performed by people of different ages and levels of fitness without any strong confrontation, and improve the sitting posture, visual control, vestibular and cerebellar organ functions in wheelchair users, especially for the rehabilitation of spinal cord injury (SCI) patients.^{3–5,16–18} Meanwhile, the number of its participants is large and the competition is highly ornamental. In addition, wheelchair curling sport is an official event of the Winter Olympic Games, and more wheelchair users will benefit from the promotion of the Olympic Games. Although wheelchair curling is important for wheelchair users in terms of physical activity and health protection, technical monitoring of wheelchair curling has not been reported nearly as much as in other curling events. Therefore, the use of advanced science and technology to monitor wheelchair curling sport skills is conducive to promoting the development of the sport event, and assisting in monitoring and analyzing the skills.

With the advent of the 5G Internet of Things (IoT) era, the potential for human intelligent wearable devices is increasing in the direction of human-computer interaction,^{19–21} such as digital intelligent venue, sports skills monitoring, health monitoring, disease prevention and control, intelligent exoskeleton, intelligent prosthesis and other human-machine interconnections.^{22–24} Besides, the flexible and wireless operation functions can avoid the issues caused by traditional rigid devices, such as binding and uncomfortable skin contact. And the integrated sensing and sensitive response capability can realize the monitoring application of collecting human micro-mechanical energy independently. More importantly, the self-powered ability ensures the stable signal transmission during operation to avoid, for example, the inconvenience of traditional power supply (too large to carry, too small to meet the needs of the application) or easy to produce electronic waste pollution and other problems.^{25–31} The triboelectric nanogenerators (TENG) have various applications to date, such as self-power supply system,³² blue energy,³³ and high-voltage power supply,³⁴ which can harvest low-frequency mechanical energy from human biomechanics and the surrounding environment.^{35–37} The TENG has advantages such as diverse material selection, low cost, portable, self-powered, and simple structure.³⁸ It can be light and soft to obtain good skin adaptability according to the research needs. Compared to existing myoelectric sensors, motion capture systems, and smart fitness mirror, TENG can monitor the motion in real time, and non-invasively outside the

¹School of Strength and Conditioning Training, Beijing Sport University, Beijing 100084, China

²Institute of Carbon Neutrality and New Energy & School of Electronics and Information, Hangzhou Dianzi University, Hangzhou 310018, China

³China Ice Sports College, Beijing Sport University, Beijing 100084, China

⁴School of Martial Arts and Dance, Shenyang Sport University, Shenyang 110102, China

⁵Physical Education Department, Northeastern University, Shenyang 110819, China

⁶Lead contact

*Correspondence: maoyupeng@pe.neu.edu.cn

<https://doi.org/10.1016/j.isci.2023.108126>



laboratory.^{39,40} It has been applied in the field of healthcare, human-computer interaction, intelligent motion prediction, and intelligent wearable devices.^{41,42}

Here, a wireless intelligent sensing system (WISS) has been developed, which includes a WF-TENG sensing port integrated with the wearable flexible triboelectric nanogenerator (WF-TENG), flexible printed circuit (FPC), a Bluetooth wireless transmitter, along with the upper computer digital signal receiving intelligent processing port. The system can monitor wheelchair curlers' curling skills and human-computer interactive simulation training in real time. Such technology can meet various purposes of daily training and entertainment. In order to ensure that WF-TENG sensing port attached on the skin surface with good adaptability and durability, TENG was encapsulated with PDMS solution to prevent the internal triboelectric layer from being affected by impurities such as sweat or dander on the skin surface. In addition, it is flexible and biocompatible for prolonged skin contact. Ecoflex film and PU film were used as triboelectric layers, which had good physical properties of tensile strength (Ecoflex) and wear resistance (PU) compared with other triboelectric materials.^{43–46} Not only does it have stable electric properties and fast response (53 ms), but it also has a long operation life. The WF-TENG can be easily attached on the skin surface of the test site, and can real-time transmit relevant sports skills information accurately through the wireless transmission system based on the WF-TENG, without interfering with sport performance and causing limb discomfort. Moreover, the upper computer digital signal receiving intelligent processing port realizes human-computer interactive application, judges and feeds back the accuracy of the pitcher by identifying the throwing information. This work enriches the application of self-powered sensors in the field of the Internet of Things and human-computer interaction. It will undoubtedly provoke the development of wearable electronic systems in the field of digital stadiums and sports assistive devices, and provide wheelchair users with new ideas for fitness exercises. More importantly, reporting on the work of wheelchair curling can draw attention to the people with disabilities within the scientific field, making the results of scientific research more universal and sustainable.

RESULTS AND DISCUSSION

Wireless intelligent sensing system

Figure 1 shows the design of the WISS for wheelchair curling skills, composing of WF-TENG, a FPC, a WF-TENG sensing port integrated with a wireless Bluetooth transmitter, and an upper computer digital signal receiving intelligent processing port. The WF-TENG sensor can be attached on the skin surface of body in a portable and non-destructive way (without damaging the skin surface) to collect low-frequency of human motion mechanical energy. During the process of collecting mechanical energy, the WF-TENG completes self-power supply, and simultaneously transmits the biological sensing signal to the upper computer in real time for digital signal reception and intelligent processing to achieve human-computer interaction and intelligent technical judgment. The purpose of this functional design is to meet the needs of daily training, sports skill monitoring and entertainment.

Figure 1A shows the working diagram of WISS. The sports technical parameters are real-time transmitted during curling and can be used for technical analysis (I). Figure 1AII is a 3D diagram of the structural design of the WF-TENG sensor end. The flexible design is designed to avoid trauma caused by rigid sensors or circuit boards rubbing against the skin during motion. The WF-TENG collects the mechanical energy of human motion to supply power to the flexible circuit terminal, and uploads the motion information to the digital signal receiving intelligent processing terminal of the upper computer for presentation. Figure 1B shows the multi-angle optical image and cross-sectional optical microscope image of the WF-TENG sensing port. Figure 1BI is the front of optical image. MCU and Bluetooth as important components of the flexible circuit port. Figure 1BII is the optical image of the WF-TENG sensing port after folding. The WF-TENG and flexible circuits both exhibit excellent folding characteristics. Figure 1BIII is the application status of optical image. It shows the WF-TENG sensing port has good fit and thinness. Figure 1BIV is the optical microscope image of WF-TENG section. It is found by scanning electron microscope that PU and Ecoflex layers are tightly wrapped together, which can minimize the influence of sweat and heavy exercise on the triboelectric layer and improve the durability. Figure 1C shows the circuit diagram of WISS flexible circuit port. After the sensor signal is generated, the waveform is processed by a filter. The MCU converts the sensing analog signal into a digital signal and wirelessly transmits it into the upper computer digital signal receiving intelligent processing port through Bluetooth with an effective communication distance of 70 m. Figure 1D shows the functional diagram of WISS. Collection and transmission of real-time sports information by WF-TENG. At the same time, the intelligent processing port of the upper computer realizes the application of human-computer interaction and judges and feeds back the sports sensing information.

Working principle of WF-TENG

Figure 2A shows the fabrication process of WF-TENG. The PU film with electrodes as a positive triboelectric layer on the PDMS substrate. And the Ecoflex film is fabricated as a negative triboelectric layer with a FEP substrate. Finally, it is encapsulated by drip-filling with PDMS solution. Figure 2B shows the working mechanism. Here, the working mechanism of WF-TENG was based on the contact-separation mode (Figure 2B). In stage I, the pitcher technical action is in the recovery storage posture, the triboelectric layers are in contact with each other, and the induction charge of equal size and opposite direction is generated on the triboelectric layer surface. In stage II, the pitcher technical action starts in push-out delivery posture, and the triboelectric layers start to separate the triboelectric layers to produce a smaller distance between them, generate an induced potential difference between the two electrodes, and electron flow from PU to Ecoflex and generate a downward current. In stage III, the curler is pushed out of the delivery pose completely, the two triboelectric layers are completely separated and the electrostatic field reaches equilibrium. In stage IV, the recycling curler continues to present a recycling pose, and the two triboelectric layers approaching the electrons will undergo a backflow to generate an upward current. When the upper and lower triboelectric layers are in complete contact, a cycle is completed.

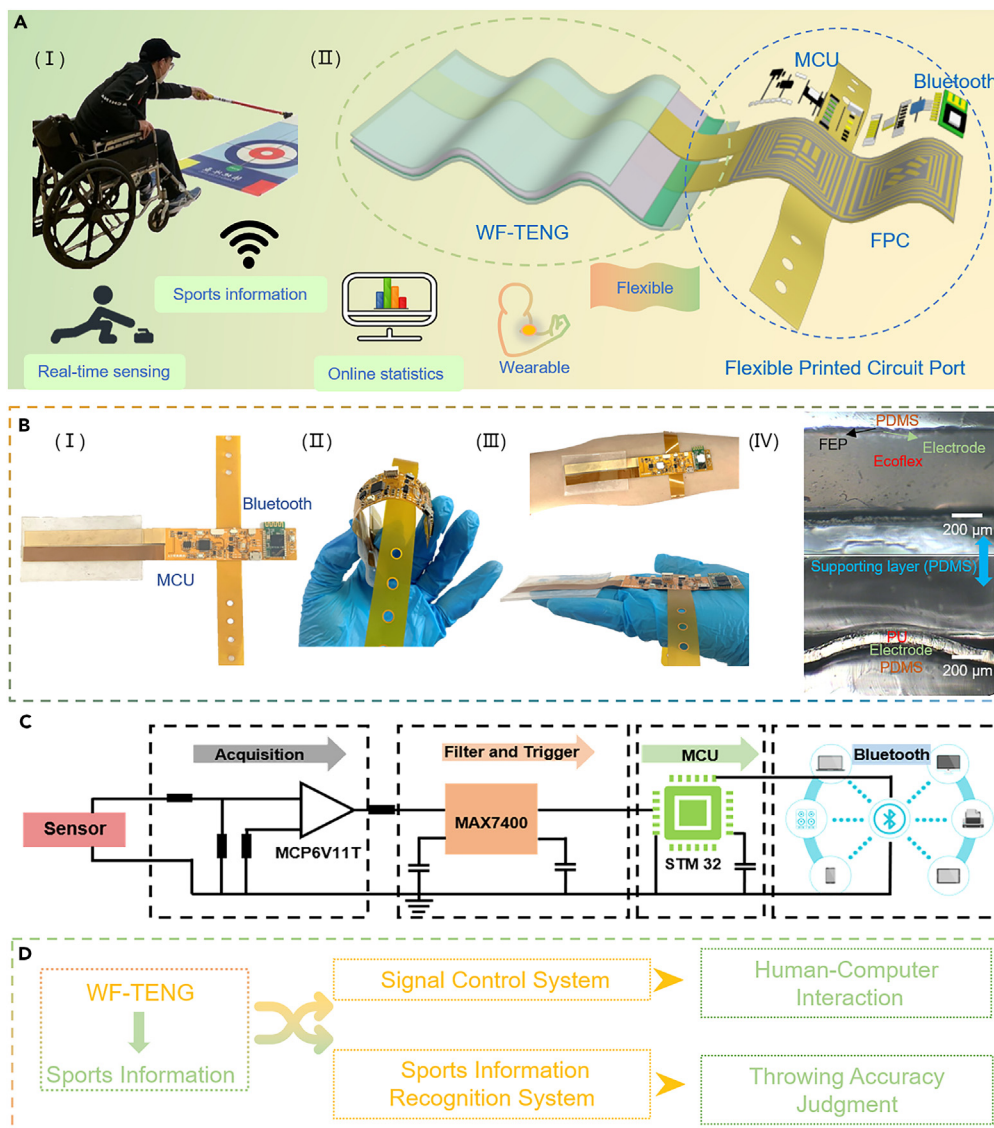


Figure 1. Design of the wireless intelligent sensing system for wheelchair curling technology

(A) Schematic diagram of wireless intelligent sensing system. (I) Optical images of wheelchair curling tester. (II) 3D drawings of the WF-TENG sensing port structure design.

(B) Multi-angle optical images and cross-sectional optical microscope images of the WF-TENG sensing port. (I) Front of WF-TENG. (II) Folded state of WF-TENG.

(III) Application state of optical image. (IV) Optical microscope images of WF-TENG section.

(C) Circuit diagram of the flexible circuit port of the WF-TENG sensing port.

(D) Functional diagram of WISS.

In order to further reveal the working mechanism of WF-TENG, its potential distribution was simulated in COMSOL software. [Figure 2C](#) reveals the potential distribution between the upper and lower electrodes with different gaps. The potential difference between the upper and lower electrodes varies with the triboelectric layer distance, showing an increasing trend. [Figure 2D](#) illustrates the voltage signal from the WF-TENG switch polarity test. The two states of forward and reverse connection press and release produce different voltage waveforms, it shows that the voltage signal is sent by WF-TENG instead of the measuring system. Its unique periodic operating mechanism and the periodic characteristic of motion matching can effectively monitor various types of sports.

Performance testing of WF-TENG

The motion of skeletal muscles helps body to accomplish displacement and move other objects. “Push and pull” are the most basic form of motion of the skeletal muscles of the upper limbs. The motion skills of wheelchair curling sport consists of a synergy between the accumulation

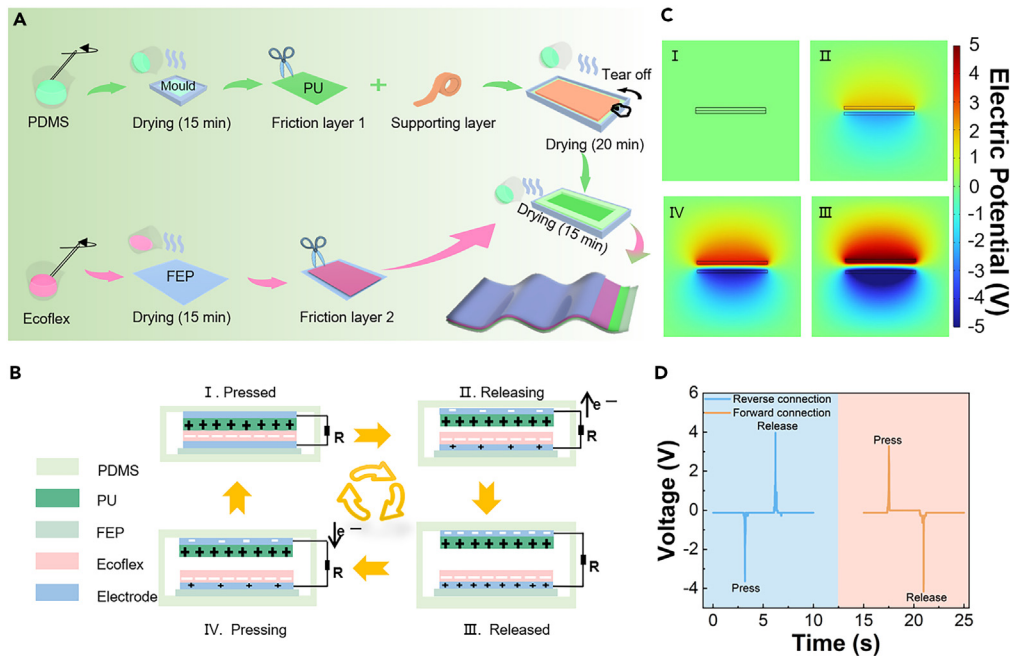


Figure 2. The production and working principle of WF-TENG

- (A) The production of WF-TENG.
- (B) WF-TENG working principle.
- (C) COMSOL simulation of WF-TENG electric potential.
- (D) WF-TENG switch polarity test.

and recovery of the skeletal muscles of the trunk and upper limbs “pull” and the throwing and releasing “push”. However, the elbow joint is the key point for monitoring the upper extremity skeletal muscle kinetic chain to control the “pull and push” that determines the accuracy of the curling throw. The WF-TENG can be attached to the body joints in a lightweight manner. The flexible WF-TENG avoids binding the range of motion of the joints during human motion. Therefore, the properties of the WF-TENG are tested using a linear motor setting program without human interference to ensure the objectivity of the data source and meet the actual motion requirements.

Figure 3 shows the performance of WF-TENG. Figure 3A shows the outputting voltage of WF-TENG under the same force, temperature, bending angle, and different frequency conditions. When the frequencies are 1.5 Hz, 2 Hz, 2.5 Hz and 3 Hz, the average outputting voltages is 4.72 V, 4.68 V, 4.72 V and 4.72 V, respectively. It shows that WF-TENG has good stability for monitoring low frequency motion. The response of WF-TENG at different frequencies is shown in Figure 3B. The response can be calculated by the following equation:

$$R\% = \left| \frac{V_i - V_0}{V_0} \right| \times 100\% \quad (\text{Equation 1})$$

The V_0 and V_i are the outputting voltage at 1.5 Hz and other frequencies, respectively. When WF-TENG are operated at 1.5 Hz, 2 Hz, 2.5 Hz and 3 Hz under the same force, temperature, bending angle and different frequency conditions, the corresponding outputting response is 0%, 0.8%, 0% and 0%, respectively. The outputting voltage of WF-TENG hardly varies with the motion frequency, indicating that the change of motion frequency can be accurately monitored during actual curling.

In order to measure the outputting voltage value of WF-TENG under different bending angles, a stepper motor was used to simulate the change of joint angle (Figure S1). The side length of triangle is 7.8 cm. The height of the triangle is determined by the set value based on the absolute motion of the stepper motor. The absolute motion value increases by 6 mm for every 0.1 triangle height increase. According to the cosine function, the bending angle of WF-TENG ($2\cos\beta$) can be calculated. Figure 3C shows the outputting voltage of WF-TENG at the same frequency (1.5 Hz) and different bending angles. When the bending angles are 45°, 75°, 104° and 125°, the average outputting voltage is 7.87 V, 5.72 V, 4.87 V and 3.1 V, respectively. The linear relationship between the WF-TENG bending angle and outputting voltage are shown in Figure S2. The calculation equation can be expressed as followings:

$$V = 10.26 - 0.06x \quad (\text{Equation 2})$$

The V is the outputting voltage (V) and x is the bending angle (°). According to the voltage value, the change of the body elbow joint angle can be derived, which provides some references for the body to adjust the elbow joint angle during the pot-throwing process. The linearity

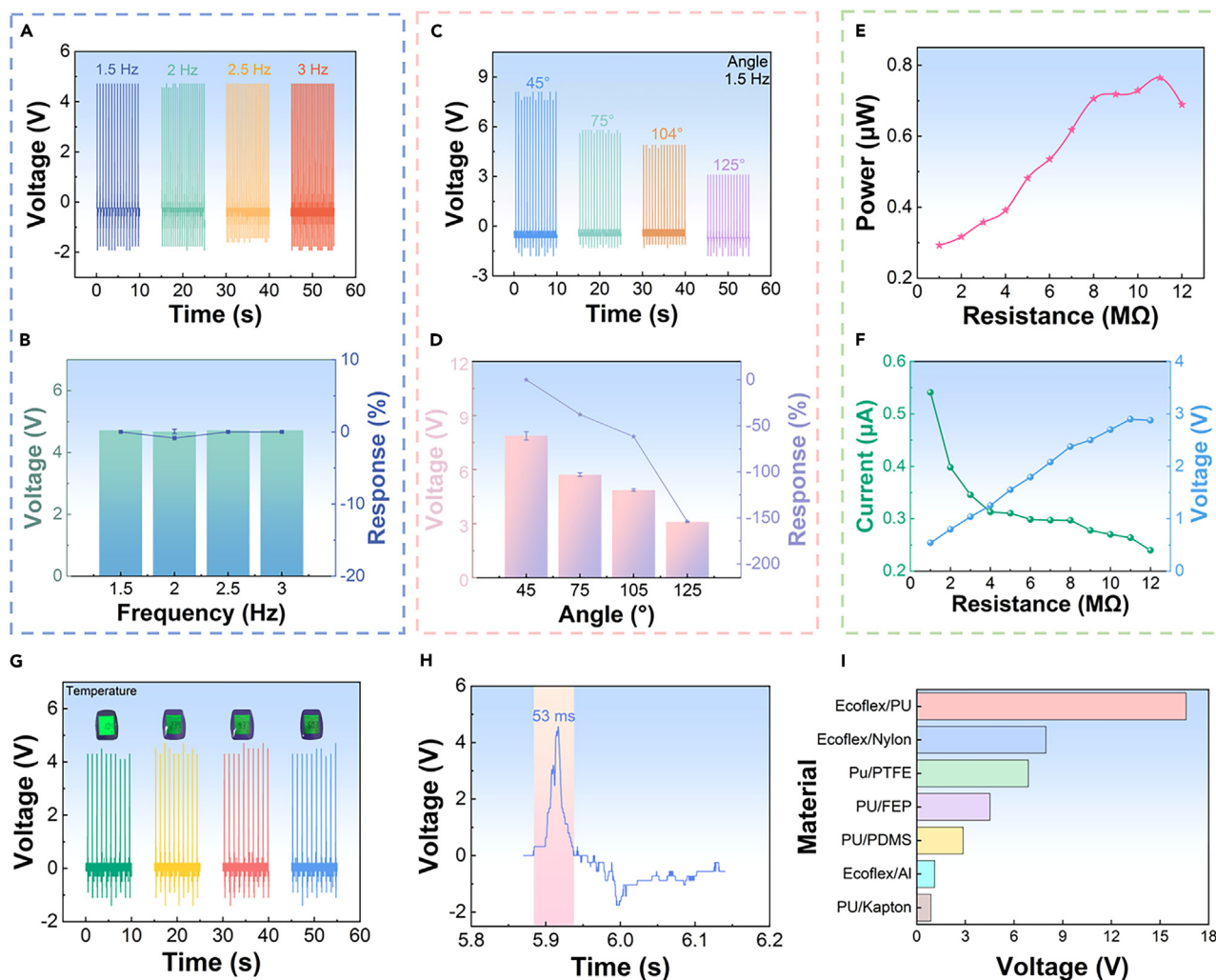


Figure 3. Performance testing and selection of WF-TENG

- (A) WF-TENG outputting voltage of different frequencies.
- (B) WF-TENG voltage response at different frequencies.
- (C) WF-TENG outputting voltage of different bending angles.
- (D) Voltage response of WF-TENG under different bending angles.
- (E) WF-TENG outputting power at different load resistances.
- (F) Outputting voltage and current of WF-TENG under different load resistance.
- (G) Outputting voltage of WF-TENG under different temperature conditions.
- (H) Real-time response of WF-TENG.
- (I) Voltage generated by the triboelectric of multiple material combinations.

value Pearson correlation coefficient $r = -0.98297$ indicates a significant correlation between WF-TENG bending angle and voltage. Figure 3D shows the voltage and response of WF-TENG at different angles. The V_0 is the outputting voltage at a bending angle of 45° and V_i is the outputting voltage at other bending angles. When the WF-TENG bending angle are 45° , 75° , 104° and 125° , the corresponding outputting response is 0%, 38%, 62% and 154% respectively. It shows that the WF-TENG can clearly and sensitively distinguish the change of bending angle during the motion. Figure 3E shows the WF-TENG outputting power at different load resistances. The maximum value of $0.76 \mu\text{W}$ is reached at a load of $11 \text{ M}\Omega$, which shows that the sensor has a resistance of $11 \text{ M}\Omega$. Figure 3F shows the WF-TENG outputting voltage and current at different load resistances. Current is calculated by using external resistances. The maximum voltage and current values are 2.9 V and $0.54 \mu\text{A}$.

In order to reveal the effect of temperature on WF-TENG, a thermal stability test was performed. Figure 3G shows the outputting voltage of WF-TENG at different temperatures. The average outputting voltage are 4.28 V , 4.44 V , 4.46 V and 4.37 V when the temperatures are 10.4°C , 23.9°C , 43.7°C and 60.3°C , respectively. Figure S3 shows that WF-TENG voltage response at different temperatures. When the

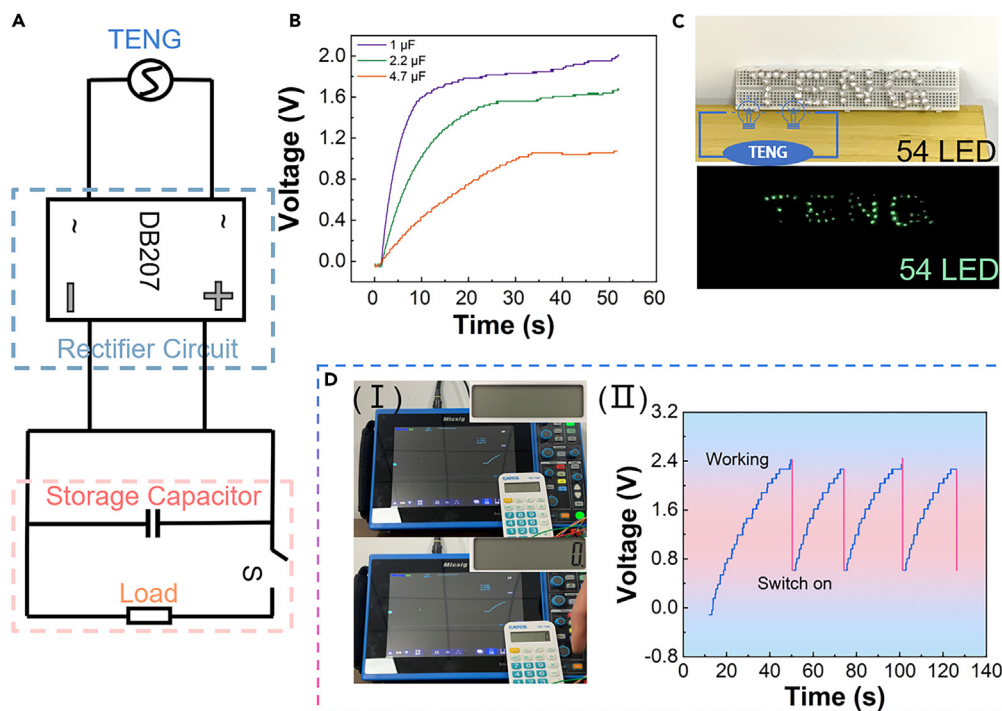


Figure 4. Triboelectric properties of WF-TENG

(A) Charge and discharge equivalent circuit diagram.

(B) Charging performance of capacitors with different loads.

(C) Tap to light up 54 commercial LEDs.

(D) WF-TENG drives a small calculator to work. (I) Optical image of driving the mini-calculator operation. (II) Charge and discharge curves.

WF-TENG temperatures are 10.4°C, 23.9°C, 43.7°C and 60.3°C, the corresponding outputting response is 0%, 4%, 2% and 2%, respectively. It indicates that the WF-TENG has good thermal stability. The average skin temperature of the human body is 33.8°C. When WF-TENG comes into direct contact with the skin, it will not affect the WF-TENG outputting voltage. Figure 3H shows the fast response time of the WF-TENG is about 53 ms. The data of throwing curling can be transmitted to the upper computer in real time for coaches to analyze and master the state of throwing pots of athletes in time. At the same time, it provides a guarantee for the signal control system to realize the man-machine interactive accuracy judgment of pot throwing. Figure S4 shows the stability test of WF-TENG for 2400 s of continuous operation. The outputting voltage of WF-TENG can be stabilized at 4.6 V during 2400 s operation, which can meet the daily training application.

Considering that different triboelectric materials have different dielectric constants, the corresponding electrical properties of TENG are also different. The outputting voltages obtained with Polyurethane (PU) materials and Kapton, Polytetrafluoroethylene (PTFE), Fluorinated ethylene propylene (FEP), and Polydimethylsiloxane (PDMS) were tested under the same experimental conditions. The Ecoflex material and three other typical materials: including Nylon, Aluminum foil and Polyurethane (PU) were also tested for the out voltages obtained under the same experimental conditions and the results are shown in Figure 3I. Since Ecoflex and PU show excellent electrical properties in the triboelectric layer, both of them were used as triboelectric layers in this paper, and a triboelectric voltage of 16.6 V was obtained on this basis. These results show that WF-TENG has good electrical properties and has great potential in self-powered sensing and self-powered systems.

Triboelectric properties of WF-TENG

The low-frequency mechanical energy collection capability of WF-TENG provides for WISS applications (Figure 4). Figure 4A shows the equivalent circuit diagram of WF-TENG. A rectifier is introduced into the circuit to convert AC to DC and the capacitor acts as an accumulator. The switch can control the switching of WF-TENG charging and discharging modes. The WF-TENG exhibits good charging performance when rapidly (51 s) charging for capacitor of 1 μF , 2.2 μF and 4.7 μF (Figure 4B). Figure 4C demonstrates that a gentle tap of WF-TENG can light up 54 commercial LEDs (Video S1). It indicates that WF-TENG has energy conversion capability. Figure 4D shows the WF-TENG driving mini calculator working. Figure 4DI is a calculator charging optical image. When the WF-TENG charges the capacitor to 2.4 V, the calculator screen lights up when the switch is pressed. After the capacitor is discharged to 0.6 V, it is not enough power to keep the calculator running. Figure 4DII shows the flow of the WF-TENG driving a small calculator for four charges and discharges, and the good charging performance of WF-TENG shows some commercial promise.

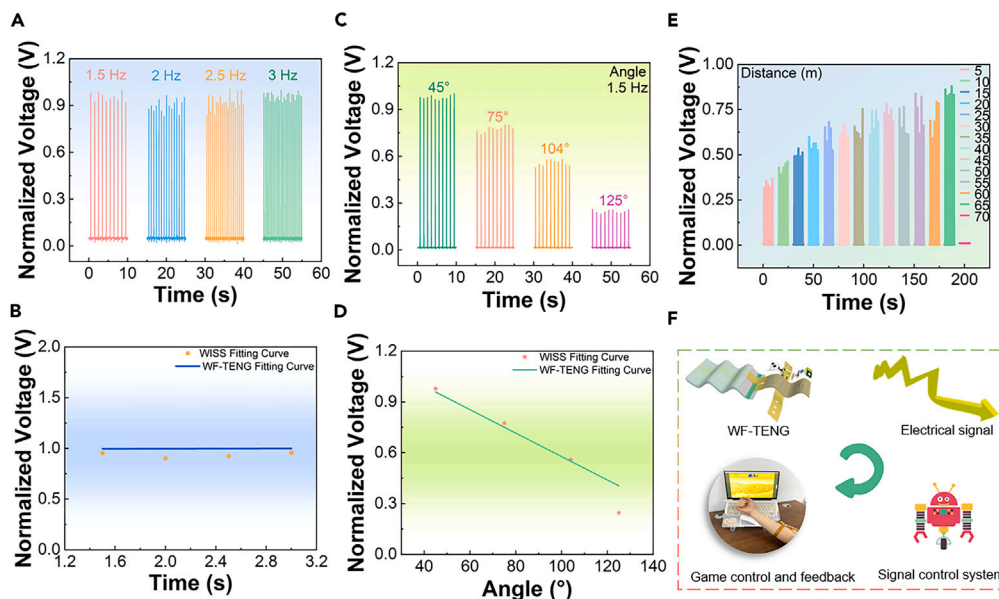


Figure 5. Applications of WISS wireless transmission and human-computer interaction

- (A) WISS outputting voltage at different frequencies.
 (B) Fitting curves of WISS and WF-TENG at different frequencies.
 (C) WISS outputting voltage at different angles.
 (D) Fitting curves of WISS and WF-TENG at different angles.
 (E) Test of WISS transmission distance.
 (F) Diagram of WISS human-computer interaction workflow.

Practical application of WISS

The WF-TENG sensing port has been proven to be flexible and lightweight in converting trace mechanical energy of human motion into electrical energy. The wireless transmission performance and human-machine interaction were performed to verify the reliability of WISS in practical applications. Figure 5A shows the normalized outputting voltage of the WISS at different frequencies. The fitted curves of the WISS wireless outputting voltage compared with the WF-TENG outputting voltage at different frequencies are shown in Figure 5B. The fitting value of WF-TENG is $r = 0.2582$, and that of WISS is $r = 0.13708$, the fitting degree between them is high, which shows that WISS can monitor different motion frequencies wirelessly. Figure 5C shows the normalized outputting voltage for different bending angles of WISS. Figure 5D shows the fitted curve of the WISS wireless outputting voltage compared with the WF-TENG for different angles. The fitting value of WF-TENG is $r = -0.98508$, and that of WISS is $r = -0.99429$, the fitting degree between them is high. The results show that WISS has good real-time monitoring ability for motion angle changes. Monitoring the changes of motion frequencies and motion angles can provide more comprehensive information to help evaluate the implementation level of sports skills. For example, adjusting the arm swing frequency and palm entry angle in swimming can affect the stroke skills, and speed skating stirrups frequency and knee leg retraction angle can affect the straight skating skills. In summary, WISS can monitor human motion frequencies and angles change in real time, providing sports technology monitoring for wheelchair curling sports.

In order to meet the practical application requirements of WISS, a wireless distance response test was conducted. Figure 5E shows the motion signal outputting during the body casual motion within a 70 m radius of the WISS. The increase in output voltage is due to the different bending angles of sensor. It is worth noting that the WISS transmission is stable within 65 m range (Video S2), which provides the possibility of wireless technology monitoring for indoor sports programs. However, wireless remote monitoring can reduce the interference to mental state and freedom of motion, which is conducive to the development of skills and tactics and collect more data for analysis and help to improve skills. In addition, we realized the human-computer interaction application for motion control training through WISS (Figure 5F). The WF-TENG acts as a sensing unit for human-computer interaction has displayed advantages of lightness, portability and low cost. The workflow of WISS human-computer interaction system mainly includes three parts. First, the WF-TENG sensing terminal converts the collected biological signals into electronic signals. Second, the signal control system encodes and identifies the signals for transmission to the upper computer. Finally, the game control and intelligent feedback are realized. The virtual game throws a hook-lock (Video S3) when the body joints are flexed, actively controlling the in-game operation through signal sensing. The simple human-computer interaction application provides an assistance to curling-specific reaction time training and enhances the training immersion experience to improve training fun, engagement and training efficiency.

WISS wheelchair sports monitoring

The wheelchair curling throwing process is controlled by the motion chain of upper limb muscles such as trunk, shoulder and wrist. The “Pulling” and “pushing” curling throwing motions drive the force to the curler to achieve Draw, Front, Freeze throwing accuracy class technique or

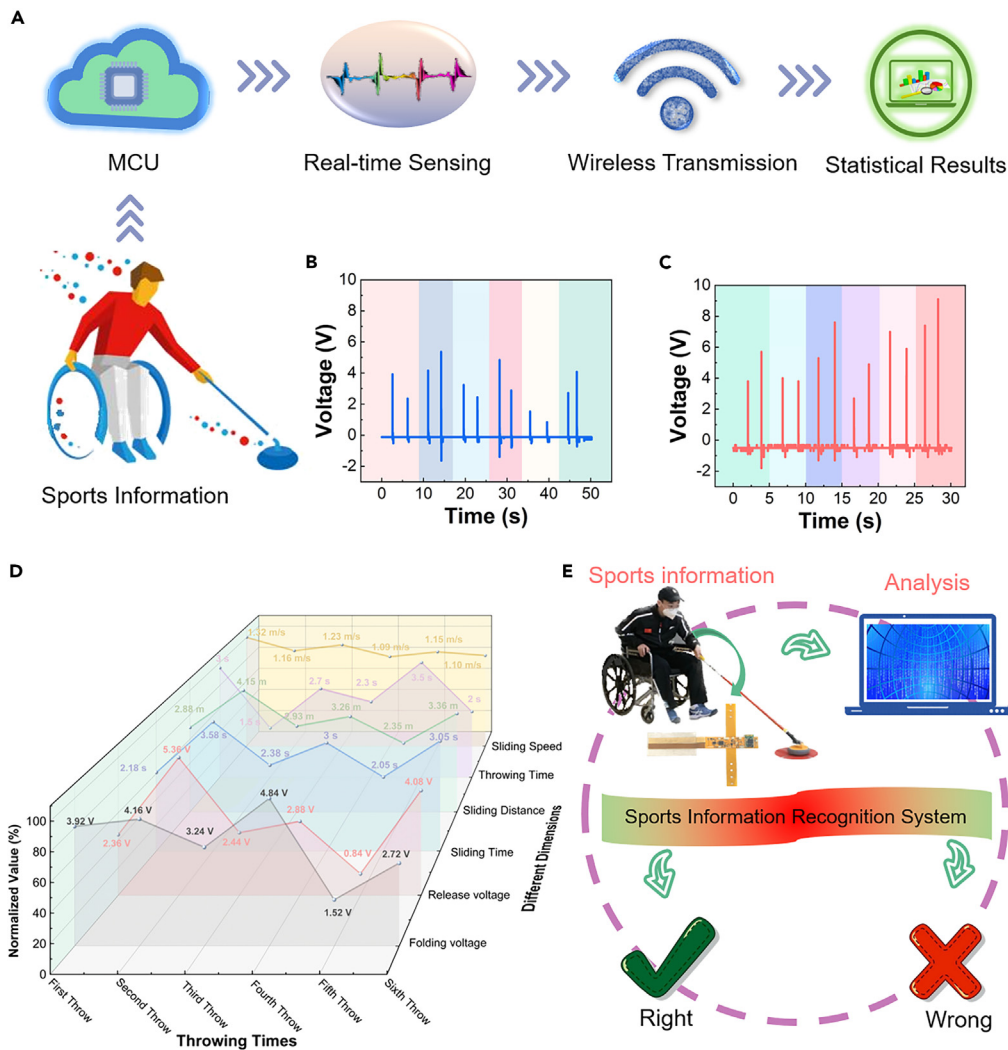


Figure 6. Application of WISS wheelchair sports monitoring

- (A) Technique analysis scheme diagram of WISS curling.
- (B) Outputting voltage of WISS curling throwing accuracy techniques.
- (C) Outputting voltage of WISS curling hit techniques.
- (D) Data collected by WISS on curling technique.
- (E) The workflow diagram of WISS upper computer intelligent technique determination.

Hit and Roll, Clearing, Double Takeout, and other hitting class techniques. However, the best place to monitor the entire power chain is the collapsible elbow joint.⁴⁷ Therefore, the WF-TENG sensing port of the WISS was attached to the tester's elbow joint to monitor the wheelchair curling throwing technique.

Figure 6A shows the workflow of WISS, where the WF-TENG sensing port converts the motion sensing signal into an electronic signal that is wirelessly transmitted to the upper computer intelligent analysis system for visualization and sports technique determination. Figure 6B shows the outputting voltage of the WISS monitoring of the tester's six throwing accuracy techniques. The single-completion pitcher technique is completed by two actions: the accumulation and retrieval "pull" and the throwing and releasing "push", thus generating two outputting voltages (Video S4). Considering that the angle change of elbow joint during pot throwing has a significant effect on the accuracy of pot throwing. Therefore, according to the bending angle calculation Equation 2 and outputting voltage, the bending angles of the six pitches were calculated as 105.67°, 101.67°, 117°, 90.33°, 145.67° and 125.67°. The tester hit the center of the red zone with the curler at an elbow flexion angle of 90.33°. Figure 6C shows the outputting voltage of the WISS monitoring of the tester's sixth curling hit techniques (Video S5). The curler hit the center of the red zone when the tester's elbow was flexed at an angle of 90.33°. Figure 6C shows the outputting voltage of the WISS monitoring of the tester's six throwing technique (Video S5). The 1st and 2nd "Raise" technique and the 4th "Wick" technique. According to the bending angle calculation Equation 2 and the folding voltage, the bending angle of the 1st, 2nd is "Raise" technique is 107.67°, 104.33°, and the bending angle

of the 4th “Wick” technique is 126° . The 3rd, 5th and 6th throws are the “Hit and Roll” technique. The 3rd, 5th and 6th “Hit and Roll” technique bends at 82.67° , 54.33° and 47.67° . The 3rd bend is large because the throwing pot stops at the expected position far from the base camp. The above results show that WISS can achieve the monitoring of the pitcher skill in the actual test.

To further understand the factors affecting the accuracy of throwing to help optimize the training method of wheelchair curling skills, we conducted a detailed analysis by using the information of six throwing techniques collected by WISS (Figure 6D). We normalized each data dimension for six throwing, and the z axis shows the normalized values of each data dimension. X and Y axes represent the number of pitches and the different pitches dimensions, respectively. As shown in the figure, during the second pot throwing, the “pull” outputting voltage of power storage recovery is 4.16 V, the “push” voltage released by throwing is 5.36 V, the throwing distance is 4.15 m, the sliding time is 3.58 s, and the throwing time is 1.5 s. Therefore, the throwing speed is the fastest and the throwing distance is the “clearing” skill. The 5th throw, with a clearly contrasting outputting voltage of 1.52 V and 0.84 V for the “pull” and “push” respectively, is the only two data that can be analyzed to show the low power of this throw, the distance of 2.35 m and the glide time of 2.05 s as well as the longer throw time (3.5 s). The longer throwing time (3.5 s) also confirms this view. This is a “Front” technique. The 4th throw was aimed at hitting the red center (Video S4). The outputting voltage at a 90.33° joint angle (4.84 V) during the recovery “pull” was significantly higher than the 2.88 V during the throw release “push”. It indicates that the tester adjusted his technique to hit the red center. However, the details of these adjustments were collected and transmitted by WISS in real time to facilitate field analysis by athletes and coaches to adjust the technique according to actual needs.

In addition, the release voltage has a good positive correlation with the sliding distance and sliding time of the curler. Coaches and athletes can analyze and determine the distance and time of sliding after curling based on the release voltage. It is worth noting that the 2nd and 5th curling sliding speeds were 1.16 m/s and 1.15 m/s, so the speed was not a limiting factor in the success of pushing action. The 2nd pitching time was the shortest at 1.5 s and the 5th pitching time was the longest at 3.5 s, but it could not be used as an absolute influencing factor for the success rate of pitching. To sum up, increasing the control of the elbow joint, increasing the stability of the elbow joint and finding the right angle of the curling shot will play a crucial role in the success rate of the push. Considering the present work, the WF-TENG sensing unit was used to monitor the information of the pitcher at the elbow joint. However, the maximum pinch velocity of the angle between the torso and the ground during the implementation of the pitcher technique, the angle of activity of the pinch, and other factors cannot be effectively monitored, and further additional research is needed in the follow-up work.

In order to display and understand the information of the tester’s throwing more intuitively, WISS has the function of motion information recognition as shown in Figure 6E. The WF-TENG sensing port transmits motion information wirelessly to the upper computer digital signal receiving intelligent processing port, and this port completes the recognition of motion information by precisely transforming the amplitude when using the Fast Fourier Transform signal inputting. The system can clearly identify the accuracy of the pitcher during the pitching process and give real-time feedback prompts in the form of animations of successes and failures by the upper computer (Video S6). The real-time feedback of motion information makes the motion data more intuitive. The development and application of this system provides new ideas for the application of wearable electronic systems in the field of digital stadiums and sports aids, and wheelchair sports.

Conclusion

In summary, a WISS has been developed. The self-powered system has the function of collecting low-frequency mechanical energy of human body for sports skills monitoring. The upper computer digital signal receiving intelligent processing port is used for wheelchair sports skills judgment prompt. By integrating wearable WF-TENG and FPC into a transmitter and combining with the reasonable design of the upper computer digital signal receiving intelligent processing port, the WISS can achieve the following functions. First, the unique filling structure can avoid the effect of impurities such as skin scales and sweat on the working performance of WF-TENG. Second, the WF-TENG sensing port does not require an external power supply for self-actuating on account of its portable, real-time and lossless collection of human motion mechanical energy. Finally, the WF-TENG collects the information of real-time sports for simple human-computer interaction applications and wheelchair sports technical judgment. This interdisciplinary research promotes the development of sports science and wheelchair sports, so that wheelchair users can have a more comfortable experience and more opportunities to participate in sports. More importantly, as a special group in society, people with disabilities should enjoy equal opportunities and resources. Reporting on the work of wheelchair curling can draw the attention to the disabilities within the scientific field, making the results of scientific research more universal and sustainable.

Limitations of the study

This study developed a WISS and applied it to monitor the skills of wheelchair curling sports. Nevertheless, two limitations must be noted. First, the multi-point information display at the intelligent processing terminal for information acquisition and upper computer signal reception integrated with multi-point control needs to be further improved. In the future, ADC multi-channel continuous scanning sampling technology should be used to achieve rapid information acquisition of multi-channel signals. Second, real-time wireless multipoint control should be used to monitor sports performance, forming a data information chain, thereby improving the quality of technical statistical analysis.

STAR★METHODS

Detailed methods are provided in the online version of this paper and include the following:

- KEY RESOURCES TABLE
- RESOURCE AVAILABILITY

- Lead contact
- Materials availability
- Data and code availability
- **METHOD DETAILS**
 - Materials
 - Preparation of flexible circuit port of the sensor
 - Preparation of WF-TENG sensor
 - Characterization and measurement
 - In the monitoring of human behaviors

SUPPLEMENTAL INFORMATION

Supplemental information can be found online at <https://doi.org/10.1016/j.isci.2023.108126>.

ACKNOWLEDGMENTS

China Ice Sports College & School of Arts, Beijing Sport University.

AUTHOR CONTRIBUTIONS

Y.M. and A.Z. conceived the idea. Y.M. initiated the study. L.C., Y.W., F.S., Y.Z., and J.W. carried out the sample preparation and characterization. Y.M. and L.C. organized the entire research. A.Z., B.L., Z.Y., R.Z., and Y.M. organized the sports scene experiment. A.Z., Y.M., B.L., and Z.Y. analyzed and interpreted the data, and wrote the article with the assistance of all other co-authors. All authors discussed the results and commented on the article.

DECLARATION OF INTERESTS

The authors declare no competing interests.

Received: April 13, 2023

Revised: July 17, 2023

Accepted: October 1, 2023

Published: October 5, 2023

REFERENCES

1. Abbafati, C., Abbas, K.M., Abbasi, M., Abbasifard, M., Abbasi-Kangevari, M., Abbastabar, H., Abd-Allah, F., Abdelalim, A., Abdollahi, M., Abdollahpour, I., et al. (2020). Global burden of 369 diseases and injuries in 204 countries and territories, 1990-2019: a systematic analysis for the Global Burden of Disease Study 2019. *Lancet* *396*, 1204–1222.
2. Pemberton, V.L., McCrindle, B.W., Barkin, S., Daniels, S.R., Barlow, S.E., Binns, H.J., Cohen, M.S., Economos, C., Faith, M.S., Gidding, S.S., et al. (2010). Report of the National Heart, Lung, and Blood Institute's Working Group on Obesity and Other Cardiovascular Risk Factors in Congenital Heart Disease. *Circulation* *121*, 1153–1159. <https://doi.org/10.1161/circulationaha.109.921544>.
3. Martin Ginis, K.A., Papatthomas, A., Perrier, M.-J., and Smith, B.; SHAPE-SCI Research Group (2017). Psychosocial factors associated with physical activity in ambulatory and manual wheelchair users with spinal cord injury: a mixed-methods study. *Disabil. Rehabil.* *39*, 187–192. <https://doi.org/10.3109/09638288.2015.1045991>.
4. Learmonth, Y.C., Rice, I.M., Ostler, T., Rice, L.A., and Motl, R.W. (2015). Perspectives on Physical Activity Among People with Multiple Sclerosis Who Are Wheelchair Users: Informing the Design of Future Interventions. *Int. J. MS Care* *17*, 109–119. <https://doi.org/10.7224/1537-2073.2014-018>.
5. Herzog, T., Swanenburg, J., Hupp, M., and Mittaz Hager, A.-G. (2018). Effect of indoor wheelchair curling training on trunk control of person with chronic spinal cord injury: a randomised controlled trial. *Spinal Cord Ser Case* *4*, 26. <https://doi.org/10.1038/s41394-018-0057-8>.
6. Powell-Wiley, T.M., Poirier, P., Burke, L.E., Després, J.P., Gordon-Larsen, P., Lavie, C.J., Lear, S.A., Ndumele, C.E., Neeland, I.J., Sanders, P., et al. (2021). Obesity and Cardiovascular Disease: A Scientific Statement From the American Heart Association. *Circulation* *143*, e984–e1010. <https://doi.org/10.1161/cir.0000000000000973>.
7. Molenaar, E.A., Hwang, S.-J., Vasan, R.S., Grobbee, D.E., Meigs, J.B., D'Agostino, R.B., Levy, D., and Fox, C.S. (2008). Burden and rates of treatment and control of cardiovascular disease risk factors in obesity - The Framingham Heart Study. *Diabetes Care* *31*, 1367–1372. <https://doi.org/10.2337/dc07-2413>.
8. Filho, J.A.O., Salvetti, X.M., de Mello, M.T., da Silva, A.C., and Filho, B.L. (2006). Coronary risk in a cohort of Paralympic athletes. *Br. J. Sports Med.* *40*, 918–922. <https://doi.org/10.1136/bjism.2006.029421>.
9. Swartz, L., Hunt, X., Bantjes, J., Hainline, B., and Reardon, C.L. (2019). Mental health symptoms and disorders in Paralympic athletes: a narrative review. *Br. J. Sports Med.* *53*, 737–740. <https://doi.org/10.1136/bjsports-2019-100731>.
10. Banks, L.M., Kuper, H., and Shakespeare, T. (2021). Social health protection to improve access to health care for people with disabilities. *Bull. World Health Organ.* *99*, 543. <https://doi.org/10.2471/blt.21.286685>.
11. Wolf, P., and Riener, R. (2018). Cybathlon: How to promote the development of assistive technologies. *Sci. Robot.* *3*, eaat7174. <https://doi.org/10.1126/scirobotics.aat7174>.
12. Matsumoto, Y., Adams, V., Jacob, S., Mangner, N., Schuler, G., and Linke, A. (2010). Regular Exercise Training Prevents Aortic Valve Disease in Low-Density Lipoprotein-Receptor-Deficient Mice. *Circulation* *121*, 759–767. <https://doi.org/10.1161/circulationaha.109.892224>.
13. Papadakis, M., and Sharma, S. (2009). Electrocardiographic screening in athletes: the time is now for universal screening. *Br. J. Sports Med.* *43*, 663–668. <https://doi.org/10.1136/bjism.2008.054874>.
14. Boraita, A., Santos-Lozano, A., Heras, M.E., González-Amigo, F., López-Ortiz, S., Villacastín, J.P., and Lucia, A. (2018). Incidence of Atrial Fibrillation in Elite Athletes. *JAMA Cardiol.* *3*, 1200–1205. <https://doi.org/10.1001/jamacardio.2018.3482>.
15. Garcia, M., Mulvagh, S.L., Merz, C.N.B., Buring, J.E., and Manson, J.E. (2016). Cardiovascular Disease in Women: Clinical

- Perspectives. *Circ. Res.* 118, 1273–1293. <https://doi.org/10.1161/CIRCRESAHA.116.307547>.
- Ellapen, T.J., Hammill, H.V., Swanepoel, M., and Strydom, G.L. (2017). The health benefits and constraints of exercise therapy for wheelchair users: A clinical commentary. *Afr. J. Disabil.* 6, 337. <https://doi.org/10.4102/ajod.v6i0.337>.
 - Lee, B.B., Cripps, R.A., Fitzharris, M., and Wing, P.C. (2014). The global map for traumatic spinal cord injury epidemiology: update 2011, global incidence rate. *Spinal Cord* 52, 110–116. <https://doi.org/10.1038/sc.2012.158>.
 - Weidner, N., Rupp, R., and Tansey, K. (2017). *Neurological Aspects of Spinal Cord Injury, 1st edition*, pp. 3–17.
 - Wei, X., Li, H., Yue, W., Gao, S., Chen, Z., Li, Y., and Shen, G. (2022). A high-accuracy, real-time, intelligent material perception system with a machine-learning-motivated pressure-sensitive electronic skin. *Matter* 5, 1481–1501. <https://doi.org/10.1016/j.matt.2022.02.016>.
 - Pu, X., An, S., Tang, Q., Guo, H., and Hu, C. (2021). Wearable triboelectric sensors for biomedical monitoring and human-machine interface. *iScience* 24, 102027. <https://doi.org/10.1016/j.isci.2020.102027>.
 - Han, J., Xu, N., Yu, J., Wang, Y., Xiong, Y., Wei, Y., Wang, Z.L., and Sun, Q. (2022). Energy Autonomous Paper Module and Functional Circuits. *Energy Environ. Sci.* 15, 5069–5081. <https://doi.org/10.1039/d2ee02557d>.
 - Khandelwal, G., Raj, N., Vivekananthan, V., and Kim, S.J. (2021). Biodegradable metal-organic framework MIL-88A for triboelectric nanogenerator. *iScience* 24, 2. <https://doi.org/10.1016/j.isci.2021.102064>.
 - Liu, Z., Zhao, Q., Zuo, Z.X., Yuan, S.Q., Yu, K., Zhang, Q., Zhang, X., Sheng, H., Ju, H.Q., Cheng, H., et al. (2020). Systematic Analysis of the Aberrances and Functional Implications of Ferroptosis in Cancer. *iScience* 23, 101302. <https://doi.org/10.1016/j.isci.2020.101302>.
 - Gunawardhana, K.R.S.D., Wanasekara, N.D., and Dharmasena, R.D.I.G. (2020). Towards Truly Wearable Systems: Optimizing and Scaling Up Wearable Triboelectric Nanogenerators. *iScience* 23, 101360. <https://doi.org/10.1016/j.isci.2020.101360>.
 - Jiang, Y., Trotsyuk, A.A., Niu, S., Henn, D., Chen, K., Shih, C.C., Larson, M.R., Mermin-Bunnell, A.M., Mittal, S., Lai, J.C., et al. (2023). Wireless, closed-loop, smart bandage with integrated sensors and stimulators for advanced wound care and accelerated healing. *Nat. Biotechnol.* 41, 652–662. <https://doi.org/10.1038/s41587-022-01528-3>.
 - Derakhshandeh, H., Kashaf, S.S., Aghabaglou, F., Ghanavati, I.O., and Tamayol, A. (2018). Smart Bandages: The Future of Wound Care. *Trends Biotechnol.* 36, 1259–1274. <https://doi.org/10.1016/j.tibtech.2018.07.007>.
 - Liu, A., Long, Y., Li, J., Gu, L., Karim, A., Wang, X., and Gibson, A.L.F. (2021). Accelerated complete human skin architecture restoration after wounding by nanogenerator-driven electrostimulation. *J. Nanobiotechnol.* 19, 280. <https://doi.org/10.1186/s12951-021-01036-7>.
 - Kekonen, A., Bergelin, M., Johansson, M., Kumar Joon, N., Bobacka, J., and Viik, J. (2019). Bioimpedance Sensor Array for Long-Term Monitoring of Wound Healing from Beneath the Primary Dressings and Controlled Formation of H₂O₂ Using Low-Intensity Direct Current. *Sensors-Basel* 19, 2505. <https://doi.org/10.3390/s19112505>.
 - Trung, T.Q., Ramasundaram, S., Hwang, B.U., and Lee, N.E. (2016). An All-Elastomeric Transparent and Stretchable Temperature Sensor for Body-Attachable Wearable Electronics. *Adv. Mater.* 28, 502–509. <https://doi.org/10.1002/adma.201504441>.
 - Wang, C., Lu, L., Li, W., Shao, D., Zhang, C., Lu, J., and Yang, W. (2022). Green-in-green biohybrids as transient biotriboelectric nanogenerators. *iScience* 25, 105494. <https://doi.org/10.1016/j.isci.2022.105494>.
 - Sun, F., Zhu, Y., Jia, C., Zhao, T., Chu, L., and Mao, Y. (2023). Advances in self-powered sports monitoring sensors based on triboelectric nanogenerators. *J. Energy Chem.* 79, 477–488. <https://doi.org/10.1016/j.jechem.2022.12.024>.
 - Hinchet, R., Yoon, H.J., Ryu, H., Kim, M.K., Choi, E.K., Kim, D.S., and Kim, S.W. (2019). Transcutaneous ultrasound energy harvesting using capacitive triboelectric technology. *Science* 365, 491–494. <https://doi.org/10.1126/science.aan3997>.
 - Huang, J., Yang, X., Yu, J., Han, J., Jia, C., Ding, M., Sun, J., Cao, X., Sun, Q., and Wang, Z.L. (2020). A universal and arbitrary tactile interactive system based on self-powered optical communication. *Nano Energy* 69, 104419. <https://doi.org/10.1016/j.nanoen.2019.104419>.
 - Cheng, J., Ding, W., Zi, Y., Lu, Y., Ji, L., Liu, F., Wu, C., and Wang, Z.L. (2018). Triboelectric microplasma powered by mechanical stimuli. *Nat. Commun.* 9, 3733. <https://doi.org/10.1038/s41467-018-06198-x>.
 - Yong, S., Wang, J., Yang, L., Wang, H., Luo, H., Liao, R., and Wang, Z.L. (2021). Auto-Switching Self-Powered System for Efficient Broad-Band Wind Energy Harvesting Based on Dual-Rotation Shaft Triboelectric Nanogenerator. *Adv. Energy Mater.* 11, 14. <https://doi.org/10.1002/aenm.202101194>.
 - Wang, Y., Liu, X., Wang, Y., Wang, H., Wang, H., Zhang, S.L., Zhao, T., Xu, M., and Wang, Z.L. (2021). Flexible Seaweed-Like Triboelectric Nanogenerator as a Wave Energy Harvester Powering Marine Internet of Things. *ACS Nano* 15, 15700–15709. <https://doi.org/10.1021/acsnano.1c05127>.
 - Zi, Y., Guo, H., Wen, Z., Yeh, M.H., Hu, C., and Wang, Z.L. (2016). Harvesting Low-Frequency (< 5 Hz) Irregular Mechanical Energy: A Possible Killer Application of Triboelectric Nanogenerator. *ACS Nano* 10, 4797–4805. <https://doi.org/10.1021/acsnano.6b01569>.
 - Luo, J., Gao, W., and Wang, Z.L. (2021). The Triboelectric Nanogenerator as an Innovative Technology toward Intelligent Sports. *Adv. Mater.* 33, 2004178. <https://doi.org/10.1002/adma.202004178>.
 - Zhu, Y., Zhao, T., Sun, F., Jia, C., Ye, H., Jiang, Y., Wang, K., Huang, C., Xie, Y., and Mao, Y. (2023). Multi-functional triboelectric nanogenerators on printed circuit board for metaverse sport interactive system. *Nano Energy* 113, 108520. <https://doi.org/10.1016/j.nanoen.2023.108520>.
 - Zhang, Q., Jin, T., Cai, J., Xu, L., He, T., Wang, T., Tian, Y., Li, L., Peng, Y., and Lee, C. (2022). Wearable Triboelectric Sensors Enabled Gait Analysis and Waist Motion Capture for IoT-Based Smart Healthcare Applications. *Adv. Sci.* 9, e2103694. <https://doi.org/10.1002/adv.202103694>.
 - Wang, L., Sun, X., Wang, D., Wang, C., Bi, Z., Zheng, L., Zhou, B., Niu, H., Wang, J., Cui, P., and Li, Q. (2023). Construction of Stretchable and Large Deformation Green Triboelectric Nanogenerator and Its Application in Technical Action Monitoring of Racket Sports. *ACS Sustain. Chem. Eng.* 11, 7102–7114. <https://doi.org/10.1021/acssuschemeng.3c00124>.
 - Sahu, M., Hajra, S., Panda, S., Rajaita, M., Panigrahi, B.K., Rubahn, H.-G., Mishra, Y.K., and Kim, H.J. (2022). Waste textiles as the versatile triboelectric energy-harvesting platform for self-powered applications in sports and athletics. *Nano Energy* 97, 107208. <https://doi.org/10.1016/j.nanoen.2022.107208>.
 - Zhao, D., Zhuo, J., Chen, Z., Wu, J., Ma, R., Zhang, X., Zhang, Y., Wang, X., Wei, X., Liu, L., et al. (2021). Eco-friendly in-situ gap generation of no-spacer triboelectric nanogenerator for monitoring cardiovascular activities. *Nano Energy* 90, 106580. <https://doi.org/10.1016/j.nanoen.2021.106580>.
 - Zhao, T., Fu, Y., Sun, C., Zhao, X., Jiao, C., Du, A., Wang, Q., Mao, Y., and Liu, B. (2022). Wearable biosensors for real-time sweat analysis and body motion capture based on stretchable fiber-based triboelectric nanogenerators. *Biosens. Bioelectron.* 205, 114115. <https://doi.org/10.1016/j.bios.2022.114115>.
 - Rongen, J.J., van Tienen, T.G., van Bochove, B., Grijpma, D.W., and Buma, P. (2014). Biomaterials in search of a meniscus substitute. *Biomaterials* 35, 3527–3540. <https://doi.org/10.1016/j.biomaterials.2014.01.017>.
 - Soldani, G., Losi, P., Bernabei, M., Burchielli, S., Chiappino, D., Kull, S., Briganti, E., and Spiller, D. (2010). Long term performance of small-diameter vascular grafts made of a poly(ether)urethane-polydimethylsiloxane semi-interpenetrating polymeric network. *Biomaterials* 31, 2592–2605. <https://doi.org/10.1016/j.biomaterials.2009.12.017>.
 - Wang, X., Liu, R., Zhang, T., and Shan, G. (2022). The Proper Motor Control Model Revealed by Wheelchair Curling Quantification of Elite Athletes. *Biology-Basel* 11, 176. <https://doi.org/10.3390/biology11020176>.

STAR★METHODS

KEY RESOURCES TABLE

REAGENT or RESOURCE	SOURCE	IDENTIFIER
Chemicals, peptides, and recombinant proteins		
Smooth-on Ecoflex 00-30	Beijing Lancheng Fan Fei Technology Co., Ltd. (Beijing, China).	N/A
PDMS	Tianjin Youheng Electronic Technology Co., Ltd. (Tianjin, China).	N/A
PU	Dongguan Jinda Plastic Insulation Material Store (Dongguan, China).	N/A
FEP	Taizhou Ranked New Materials Co., Ltd. (Taizhou, China).	N/A
Software and algorithms		
Origin 2022	OriginLab	N/A
Autodesk 3ds Max	Autodesk	N/A
COMSOL Multiphysics 6.0	COMSOL	N/A

RESOURCE AVAILABILITY

Lead contact

Yupeng Mao (maoyupeng@pe.neu.edu.cn).

Materials availability

Materials used in the study are commercially available.

Data and code availability

- All data reported in this paper will be shared by the [lead contact](#) upon reasonable request.
- No new code was generated during the course of this study.
- Any additional information required to reanalyze the data reported in this paper is available from the [lead contact](#) upon reasonable request.

METHOD DETAILS

Materials

Smooth-on Ecoflex 00–30 was purchased from Beijing Lancheng Fan Fei Technology Co., Ltd. (Beijing, China). PDMS solution and curing agent were purchased from Tianjin Youheng Electronic Technology Co., Ltd. (Tianjin, China). Polyurethane (PU) film was purchased from Dongguan Jinda Plastic Insulation Material Store (Dongguan, China). Fluorinated ethylene propylene copolymer (FEP) film was purchased in Taizhou Ranked New Materials Co., Ltd. (Taizhou, China). Enameled wire was purchased from Wuhu Airite Electromechanical Equipment Co., Ltd. (Wuhu, China). Meifeng Glue was purchased from Taobao. The rectifier bridge, LEDs and capacitors were purchased from Taobao.

Preparation of flexible circuit port of the sensor

The hardware modules consisted of an operational amplifier, a filter, an MCU module, a Bluetooth module and a flexible printed circuit (FPC). In this study, firstly, Multisim was used to design and simulate the signal acquisition circuit. Secondly, after the simulation of signal acquisition circuit ran successfully, JLC EDA was used to design the schematic diagram of the signal acquisition board and PCB file. Thirdly, various components were integrated into FPC and were soldered by SMT chips. Finally, FPC is programmed and debugged to achieve the functionality we need. The generated voltage signal was transformed by an operational amplifier and filter into the measurement range of the ADC of the MCU. MCU read the data collected by the internal ADC and transmitted it wirelessly to the upper computer via the Bluetooth module for data analysis.

Preparation of WF-TENG sensor

Firstly, the two parts A and B were mixed in a 1:1 ratio, stirred by an ultrasonic mixer for 10 min, and uniformly dripped onto the FEP film with after heating at 80°C for 15 min to obtain Ecoflex films. Then, the PDMS solution was mixed with the hardener in a 10:1 ratio, stirred in an

ultrasonic mixer for 10 min, poured into the mold and heated at 80°C for 15 min to obtain the PDMS film substrate. Next, the electrode parts of flexible printed circuit (FPC) were pasted onto the PU and Ecoflex surfaces, respectively. For fabricating WF-TENG sensor, PU with electrodes was glued on the PDMS substrate as a positive triboelectric layer. A suitably sized seam sealant was glued to the surface of the PU with the purpose of constructing a support void. The PDMS solution was poured until it had been completely encapsulated and heated at 80°C for 15 min before the seam sealant was removed to form the support space. And the Ecoflex film was tightly bonded to the support layer to form a negative triboelectric layer with the FEP film port facing upward. Finally, the PDMS solution was dripped onto the FEP and placed in an oven at 80°C for 20 min to make a complete WF-TENG with sizes of 7.9 cm × 4.9 cm × 0.5 cm.

Characterization and measurement

A stepper motor with amplitude and frequency control system was used to simulate the motion of human joints. The oscilloscope (sto1102c, micsig) produced in China was used to collect the signal generated by WF-TENG and measure the electrical performance of WF-TENG.

In the monitoring of human behaviors

The experimental protocol adhered to the regulations of the Animal and Human Experimentation Committee of Northeast University (NO:2023-02566). Wheelchair curling testers were recruited from Northeast University and had been informed consent prior to testing. The collapsible elbow area is the best monitoring position for the entire power chain of wheelchair curling. Therefore, the WF-TENG sensing port was attached to the testers' elbow during the testing process and wirelessly connected to the upper computer system to monitor the wheelchair curling throwing skills. The testers then performed 12 practical tests to assess curling accuracy and "Takeout skills". The WF-TENG sensing port monitored the tester's elbow sports skills motions and the upper computer system collects real-time sports data such as folding and release voltages from the "pull" and "push" sports skills during the wheelchair curling throwing process. The release voltage is used to analyze the distance and time for curling to slide. The folding voltage is used for calculating the bending angle of the elbow joint. Based on the obtained sports data, different types of wheelchair curling skills can be judged. The same method was utilized for both wheelchair curling testers during the curling accuracy test.